Investigation on Sensor Fault Effects of Piezoelectric Transducers on Wave Propagation and Impedance Measurements

Inka Buethe[*1] and Claus-Peter Fritzen[1]
[1]University of Siegen, Institute of Mechanics and Control Engineering-Mechatronics
*Corresponding author: Paul-Bonatz-Strasse 9-11, 57076 Siegen, Germany, inka.buethe@uni-siegen.de

Abstract: Piezoelectric transducers, also called piezo wafer active sensors (PWAS) are deployed in structural health monitoring (SHM) systems. They are used as actuators and sensors for methods of structural damage detection based on acousto-ultrasonics (AU). This paper focuses on the effects that possible sensor faults, like debonding or element breakage, have on the wave propagation. It also considers the electro-mechanical impedance spectrum and its changes due to sensor damage. A COMSOL model is built, which is used for the detailed contemplation of the PWAS behavior in frequency and time domain. It is also compared to experimental results, showing the outstanding ability of the numerical model to illustrate the physical behavior in both domains.

Keywords: Structural Health Monitoring (SHM), Sensor Faults, PWAS, PZT, Electro-Mechanical Impedance (EMI), Wave Propagation, Acousto-Ultrasonics (AU)

Figure 1. Example of an aircraft fuselage equipped with a structural health monitoring (SHM) system (©Randy Montoya, share.sandia.gov).

1. Introduction

The employment of a large number of embedded sensors in advanced monitoring systems becomes more common enabling in-service detection and localization of defects as well as the assessment of defect type and extent in mechanical, civil and aerospace structures (Figure 1). The automated monitoring with permanently attached sensor systems is referred to as Structural Health Monitoring (SHM). One popular sensor type for passive and active monitoring technologies is the piezoelectric wafer active sensor (PWAS), due to its multi-purpose application as actuator and sensor and its low cost. It is used to generate a wave field, which interacts with the structure and is recorded by a second set of PWASs. From the recorded signals, different methods are used to evaluate whether the structures health state has changed. A collection of these methods can be found in Ostachowicz and Güemes [1]. Many of those methods use frequencies above 20 kHz and are gathered as acousto-ultrasonics (Figure 2).

Generally the use of sensors requires that those are functioning correctly. This is especially important when long-term monitoring (e.g. several years) is performed, because the sensor might be the weakest part of the monitoring system. A variety of transducer damages can influence the PWAS performance, e.g. degradation of the piezoelectric material or the adhesive bonding layer, debonding of the element from the structure or breakage of the element [2].

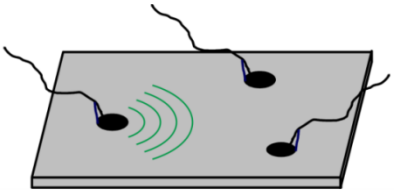

Figure 2. Basic idea of acousto-ultrasonics: With the help of a piezoelectric transducer a guided wave is generated, which interacts with the structure and is recorded by sensing transducers.

All these damages have a different effect on the wave propagation generated by the PWAS. These effects might lead to a misinterpretation of the signals followed by false information about the structural state. Studies on how to reduce this influence are already available mainly dealing with the signal processing method [3]. In this work, the generated wave field is studied enabling a physics-based statement on the effects of sensor faults on the SHM system's performance. Moreover the electro-mechanical impedance (EMI) spectrum, namely the susceptance as imaginary part of the reciprocal of the EMI, will be analyzed with respect to influences of these effects, as this spectrum is used as a tool to detect those [4], [2]. The EMI combines mechanical and electrical quantities, including the energy transfer from electrical to mechanical energy and vice versa and is therefore interesting in this context.

2. Theoretical Background

The piezoelectric effect couples electrical and mechanical energy via the piezoelectric constitutive equations, which are given here in cylindrical coordinates r-θ-z. The resulting expansion of a piezoelectric transducer element causes the attenuation of a ultrasonic wave, when a voltage signal is applied to the PWAS.

$$S_{rr} = s_{11}^{E} T_{rr} + s_{12}^{E} T_{\theta\theta} + d_{31} E_z, \quad (1)$$

$$S_{\theta\theta} = s_{12}^{E} T_{rr} + s_{11}^{E} T_{\theta\theta} + d_{31} E_z, \quad (2)$$

$$D_z = d_{31}(T_{rr} + T_{\theta\theta}) + \epsilon_{33}^{T} E_z, \quad (3)$$

where S_{rr} and $S_{\Theta\Theta}$ are components of the strain tensor, D_z is the electrical flux and E_z is the exciting electric field. The components of $\underline{\underline{s^E}}$ (e.g. s_{11}^E) are components of the compliance tensor, in which indices $rr, \Theta\Theta, r\Theta$ are replaced by $11, 22, 12$ because the piezoelectric element is assumed in-plane isotropic. T_{rr} and $T_{\Theta\Theta}$ are normal stresses. $d_{31} = d_{32}$ is the piezoelectric coefficient describing the electro-mechanical coupling between z and r respectively between z and Θ direction. ϵ_{33} is the dielectric constant.

The general characteristics and distribution of this ultrasonic wave in a guiding thin medium, as a plate like structure, can be calculated with the help of differential equations, described e.g. by Rose, [5].

The electro-mechanical impedance (EMI) includes mechanical influences of the PWAS, the adhesive layer and the structure, as well as electrical influences of the PWAS material. The susceptance, as the imaginary part of the EMI's reversal is of particular interest, as it can be used to detect sensor faults. It can be calculated via integrating the electric flux over the PWAS surface and division by the applied voltage. It is a function of frequency and can be therefore presented as spectrum. Different analytical models for the EMI calculation exist, see [6], [7], [4].

Many methods of modeling the resulting wave field are on based models, which replace the multiphysics coupling effect by a mechanical force in the first place. This procedure shows good results, when the focus is placed on the wave field and its structural interaction.

For the analysis of the effect, PWAS failure might have on the generated wave field, this procedure is not applicable at all. It is therefore necessary to model the multi-physics coupling including the constitutive equations.

In this way with basically the same model, the generated wave field as well as the electro-mechanical impedance can be calculated.

Many damage detection strategies, which are used in SHM systems employing guided waves, use correlation-based approaches. These methods use a baseline measurement, which shows, how the wave interacts with the structure at its pristine stage. Afterwards new measurements are compared to the baseline measurement, to gain information about the structural state. If the gained signal has changed, the interaction of the wave with the structure has changed. Assuming that the same wave field is generated by the actuating PWAS, it can be presumed, that the structure has changed due to damage. To compare the baseline measurement with some new measurement, the calculation of correlation coefficients is a very effective way. Nevertheless, correlation is also high, if the two signals, compared, have the same pattern but different amplitudes.

3. Numerical Model

To be able to understand, how the wave field is changed by the afore mentioned transducer damages, within this paper the multi-physics interaction of the undamaged or damaged PWAS

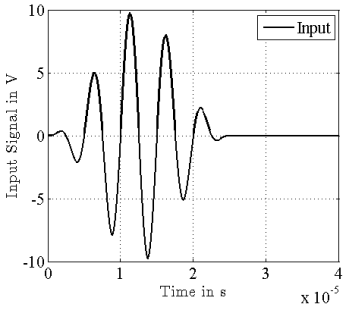

Figure 3. Excitation Signal.

and the structure is modeled in time and frequency domain. This way the effects on the electro-mechanical impedance and on the generated wave field are investigated.

The physics-based model consists of a circular piezoelectric element bonded by an adhesive layer on an isotropic structure. In the time domain a 5 cycle windowed sine wave with a central frequency of 200 kHz, as a typical signal deployed in AU, is used as actuating voltage signal.

The displacement field generated by the PWAS is analyzed at four points equally distributed around the PWAS' radius at a distance of 20 mm from its center. These points are shown in Figure 4, including the color coding used for the following displacement figures.

In the frequency domain, the electro-mechanical interaction within a frequency range from 200 to 800 kHz is examined by applying a sine signal with different frequencies within this range to the transducer. The electric flux is used to calculate the EMI. A fine mesh was used, including an O-grid to mesh the transducer itself (Figure 5).

A PWAS of diameter 6.35 mm with a thickness of 2.54 mm, attached to an aluminum plate of 2 mm thickness is modeled. To avoid edge reflection influences, and solely compare the effect of the PWAS state, the plate dimension was chosen as 250 mm and the PWAS was placed in the center of the plate. As exemplary piezoelectric constants values according to PIC 151 from PI Ceramics have been taken for the model.

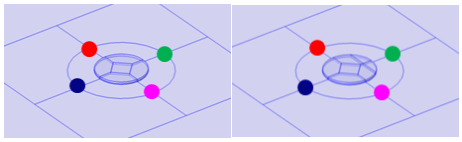

Figure 4. Location of data evaluation points with respect to the PWAS, including color coding.

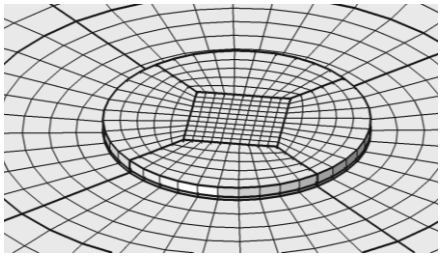

Figure 5. Mesh of the PWAS with the help of an o-grid.

3.1 Baseline – Healthy PWAS

The baseline model includes almost 500 000 degrees of freedoms, consisting of 13 302 domain elements, 26 658 boundary elements, and 1 676 edge elements.
The evaluation in the time domain of the displacements indicates, that the modeled transducer generates an axisymmetrically distributed wave field. The signal of the displacement in z-direction does not show any difference between the four points (Figure 6).

The susceptance frequency spectrum displays an even slope only interrupted around 500 kHz showing some resonance behavior of the PWAS and a generally smooth curve (Figure 11).

3.2 Debonded PWAS

To model the debonding, approx. 25% of the area of the adhesive layer has been removed under one side of the PWAS. The mesh of the irregular part was constructed with tetrahedral elements.

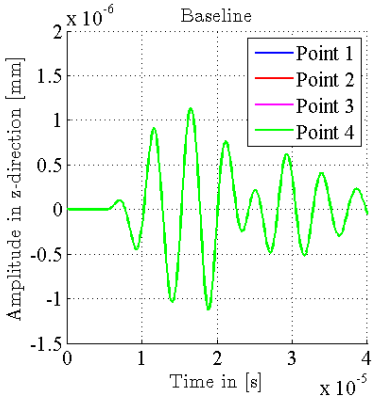

Figure 6. Time domain signal of the displacement in z-direction on the plate surface at pristine state PWAS, all evaluated points show the same signal.

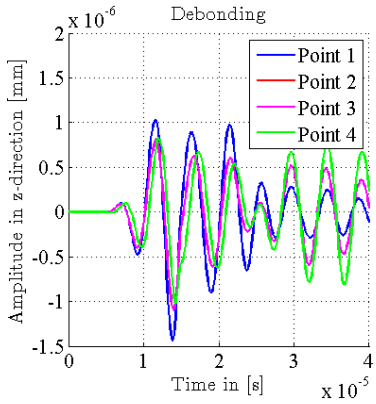

Figure 7. Time domain signal of the displacement in z-direction on the plate surface at partially debonded PWAS, the signals amplitude at the evaluated points varies significantly.

For this damage case, the calculated signal for the displacement in z-direction does not only vary due to some general change in amplitude, but the whole wave propagation picture changes (Figure 7). The evaluated points differ from each other as well as from the baseline data. Interestingly, in comparison with the baseline data it turns out that even approx. 30% higher amplitudes occur (point 1). Moreover, a longer excitation seems to be present. Both these effects can be explained, when looking at the displacement field of the debonded PWAS itself. The debonded part is not limited by the attachment to the structure and therefore produces larger motion (Figure 8). Its oscillations do not directly decline with the end of the actuation (Figure 9). This phenomenon results in additional signal power and duration in a certain direction of the generated wave field.

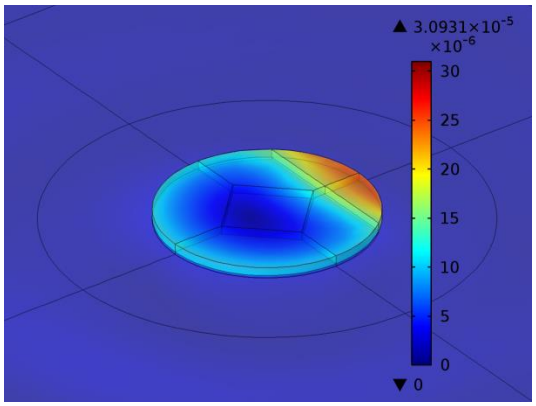

Figure 8. In-plane displacement of the debonded PWAS at time $t=1.4\cdot10^{-5}$ s.

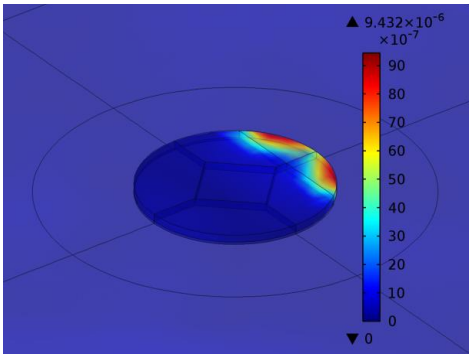

Figure 9. In-plane displacement of the debonded PWAS at time $t=2.5\cdot10^{-5}$ s.

The maximum in-plane displacement of the PWAS at time $t=2.5\cdot10^{-5}$ s (after excitation is finished) is below almost $1\cdot10^{-5}$ mm, compared to $1.5\cdot10^{-7}$ mm for the pristine PWAS. This shows that wave motion is still present in the PWAS, which can be transferred to the structure.

Regarding the susceptance spectrum also a change is visible (Figure 11). Especially in the first frequency range below the resonance the slope has increased. Moreover the behavior in the range of the resonance phenomenon shows a slightly different behavior, as well as this range is shifted to lower frequencies.

3.3 Broken PWAS

To model the breakage a piece of material was removed from the transducer, leaving the whole adhesive contact layer intact. Tetrahedral elements were used for the meshing of the irregular part.

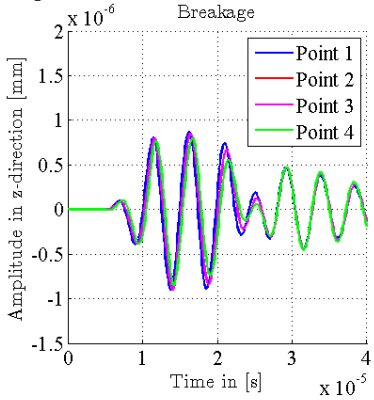

Figure 10. Time domain signal of the displacement in z-direction on the plate surface at partially broken PWAS, the amplitude of the signal at all evaluated points decreases significantly.

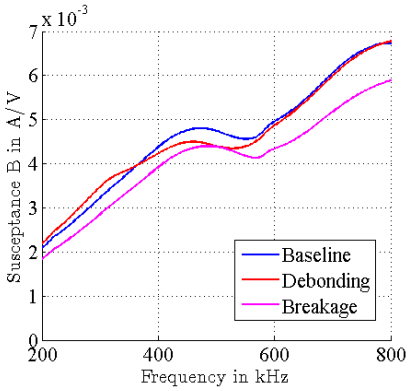

Figure 11. Comparison of the susceptance for different transducer damage states for a frequency spectrum from 200 to 800 kHz.

In the time domain, especially a loss in signal amplitude for the displacement of the plate's surface in z-direction can be recognized. The four evaluated signals only vary slightly between each other, but the maximum amplitude is reduced by more than 20%. The general waveform is not changed significantly (Figure 10).
The maximum in-plane displacement of the PWAS at a time $t=2.5\cdot10^{-5}$ s (after attenuation is finished) is below $4\cdot10^{-7}$ mm, showing that no kinetic energy is stored in the PWAS.

In the frequency domain, this transducer failure is resulting in a decreased slope for the whole frequency spectrum. Nevertheless the resonance characteristic is located at similar frequencies (Figure 11).

4. Experimental Validation

To validate the numerical model the baseline setup was experimentally investigated in detail. With the help of a laser vibrometer the out-of-plane velocity is recorded after a transducer has been actuated. Additionally, the electro-mechanical impedance spectrum was recorded.

4.1 Experimental Setup

An aluminum plate of size 500 mm x 500 mm was adjusted in an x-y table. It is assumed that the upper clamping is far enough from the PWAS to eliminate an influence on the wave field. On the plate a PWAS with a diameter 10 mm and a thickness of 0.25 mm type PIC 151 from PI instruments was bonded. A 1-D dimensional Laser Doppler Vibrometer CLV700 from Polytec was used for the recording of the out of plane velocity.

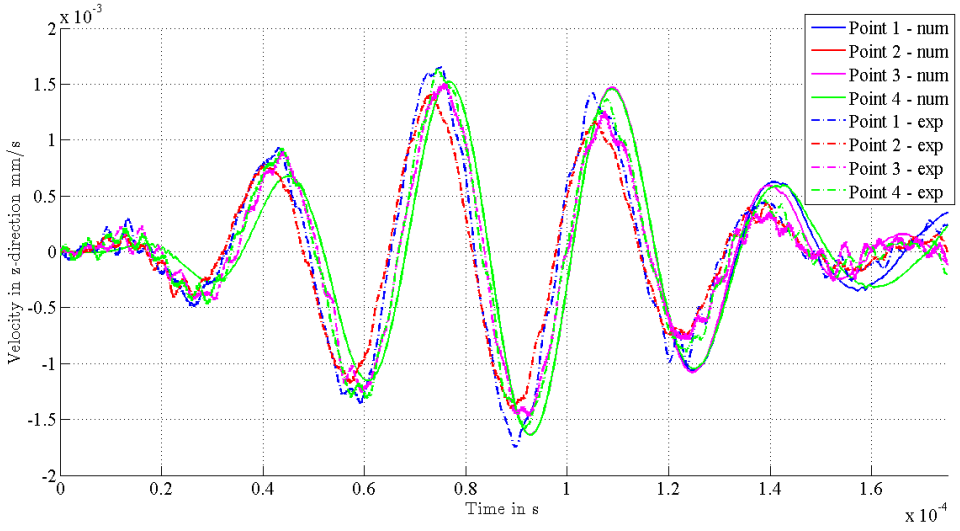

Figure 12. Comparison of the out-of-plane velocity caused by an excited transducer with a windowed 5 cycle 30 kHz sinusodial signal.

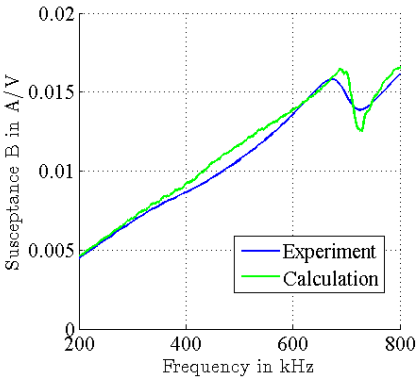

Figure 13. Comparison of the susceptance for numerical calculation and experiment for a frequency spectrum from 200 to 800 kHz.

4.2 Experimental Results

In the time domain the comparison of experimental and numerical results for a carrier frequency of 30 kHz is shown (Figure 12). The susceptance spectrum is presented for numerical calculation and experimental investigation in a frequency range of 200 to 800 kHz (Figure 13).

The experimental results show a good agreement with the results of the numerical model for the baseline measurements regarding the EMI spectrum and the generated wave field. Nevertheless it has to be mentioned, that the real world transducers show an angular dependency in the propagation behavior, see also [8], caused by the wrapped electrode. This electrode was not included in the numerical models and therefore this effect is not visible in the calculation.

5. Discussion

All studied damage scenarios have some impact on the generated wave field and the EMI spectrum. The modeling with COMSOL makes it possible to show, how different effects, which can be seen in the measureable quantities, can be explained.

For the group of acousto-ultrasonic damage detection methods, based on correlation coefficients, it is visible, that the failure of debonding has a much higher impact on the usability of the signals for structural damage detection, than a breakage has. This is caused by the change of the propagation behavior in general and the very significant difference of the signals at different radial positions. Remarkably the breakage failure assumed to have the higher impact, only shows slight variations in radial direction.

Nevertheless many acousto-ultrasonic methods (e.g. amplitude dependent methods) can not deal with both of the signal changes, caused by the different PWAS faults. It is therefore important, that both can be seen in the susceptance spectrum. This shows, that the susceptance is indeed a very useful quantity to be used for the check of PWAS.

The comparison with experimental results gained from PWAS attached to an aluminium plate shows the good quality of the multiphysics model.

6. Conclusions

The investigation shows, how important it is to check that employed PWAS are intact, as transducer faults have a big effect on the generated wave field, which is used in the Structural Health Monitoring process of acousto-ultrasonics. By explaining the reason for effects in the wave propagation, the presented multiphysics model increases the knowledge about processes that are caused by sensor faults.

7. References

[1] W. Ostachowicz and J. A. Güemes, *"New Trends in Structural Health Monitoring"*, Udine: Springer, 2013.

[2] I. Buethe and C.-P. Fritzen, "Sensor Performance Assessment Based on a Physical Model and Impedance Measurements," *Key Engineering Materials*, **vol. 570**, pp. 751-758, 2013.

[3] K. R. Mulligan, N. Nicolas Quaegebeur, P.-C. Ostiguy, M. P. and L. S., "Comparison of metrics to monitor and compensate for piezoceramic debonding in structural health monitoring," *Structural Health Monitoring*, **vol. 12(2)**, pp. 153-168, 12 2012.

[4] G. Park, C. R. Farrar, F. L. di and S. Coccia, "Performance assessment and validation of piezoelectric active-sensors in structural health monitoring," *Smart Materials and Structures*, **vol. 15**, pp. 1673-1683, 2006.

[5] J. L. Rose, *"Ultrasonic Sound in Solid*

Media", Cambridge: Cambridge University Press, 2004.

[6] V. Giurgiutiu, *"Structural Health Monitoring with Piezoelectric Wafer Active Sensors"*, Elsevier Science & Technology, 2007.

[7] S. Bhalla and C. K. Soh, "Electromechanical Impedance Modeling for Adhesively Bonded Piezo-Transducers," *Journal of Intelligent Material Systems and Structures*, **vol. 15**, pp. 955-972, 2004.

[8] J. Moll, M. V. Golub, E. Glushkov, N. Glushkov and C.-P. Fritzen, "Non-axisymmetric Lamb Wave Excitation by Piezoelectric Wafer Active Sensors," *Sensors and Actuators: A. Physical.*, **vol. 174**, pp. 173-180, 2012.